HHS Public Access

Author manuscript

*Angew Chem Int Ed Engl*. Author manuscript; available in PMC 2015 December 22.

Published in final edited form as:

*Angew Chem Int Ed Engl*. 2014 December 22; 53(52): 14419–14423. doi:10.1002/anie.201408219.

# An Upconversion Nanoparticle with Orthogonal Emissions Using Dual NIR Excitations for Controlled Two-way Photoswitching

**Jinping Lai**, **Yixiao Zhang**[†], **Nicholas Pasquale**[†], and **Ki-Bum Lee**

Department of Chemistry and Chemical Biology, Rutgers University, Piscataway, NJ 08854, TEL: (+1)848-445-2081, FAX: (+1)732-445-5312, http://rutchem.rutgers.edu/~kbleeweb/

Ki-Bum Lee: kblee@rutgers.edu

## Abstract

Developing multicolor upconversion nanoparticles (UCNPs) with the capability of regulating their emission wavelengths in the UV to visible range in response to external stimuli can offer more dynamic platforms for applications in high resolution bio-imaging, multicolor barcoding and driving multiple important photochemical reactions, such as photoswitching. In this communication, we have rationally designed single crystal core-shell structured UCNPs which are capable of orthogonal UV and visible emissions in response to two distinct NIR excitations at 808 and 980 nm. The orthogonal excitation-emission properties of such UCNPs, as well as their ability to utilize low power excitation, which attenuates any local heating from the lasers, endows the UCNPs with great potential for applications in materials and biological settings. As a proof of concept, the use of this UCNP for the efficient regulation of the two-way photoswitching of spiropyran by using dual wavelengths of NIR irradiation has been demonstrated.

### Keywords

upconversion nanoparticles; core-shell nanoparticles; two-way photoswitching; dual NIR excitations

Lanthanide-doped upconversion nanoparticles (UCNPs) have recently gained much attention due to their unique capability of upconverting low energy near-infrared (NIR) light to high energy ultraviolet (UV) and visible light.[1] Combined with other excellent photo-physical properties, including long emission lifetimes, narrow emission band-widths, and high photostability, UCNPs have shown widespread application in fields ranging from bio-imaging and sensors to photovoltaics and solid-state devices.[2] One of the critical requirements for harvesting their full potential is to develop UNCPs with emission profiles specifically tuned towards their target applications. This includes synthesizing UCNPs with strong UV emission to trigger chemical reactions such as the photocleavage of photolabile groups,[3] and highly visible emitting UCNPs for nanomedicine-based applications such as photodynamic therapy (PDT),[4] as well as NIR emitting UCNPs for *in vivo* bio-imaging.[5]

Correspondence to: Ki-Bum Lee, kblee@rutgers.edu.

[†]These authors have contributed equally to this manuscript

Among the developed various UCNPs with tailored emission profiles, multicolor UCNPs capable of regulating their emission wavelengths from the UV to visible range in response to external stimuli are garnering much interest recently, as they can offer more dynamic platforms for applications in high resolution bio-imaging, multicolor encoding and photoswitching.[6] However, there are few reports on such multicolor UCNPs. Of them, one typical example is the excitation-responsive UCNP, whose emission can be modulated between spectrally pure visible light and mixed UV/Vis emissions by changing the power density of 980 nm NIR excitation.[6b–d] This unique property of the UNCPs was then successfully applied toward driving important chemical reactions and their subsequent applications such as the two-way photoswitching of dithienylethene,[6b] the reversible control over the reflection of liquid crystals[6c] and modulating the biocatalytic activity of bacteria[6d]. However, the use of high power 980 nm NIR light in such UCNP systems, although advantageous, has been shown to cause severe local heating, which has detrimental effects on both solid-state devices and biological systems.[7] Moreover, the spectrally mixed UV/Vis emission of these UCNPs compromises the photoswitching system's ability to reliably encode and transmit information in a spatiotemporally controlled manner. Thus, to overcome these limitations, there is a clear need to develop multicolor UCNPs capable of selectively generating spectrally resolved emissions in the UV and visible regions using external stimuli with negligible heating effects.

We herein describe the design and synthesis of a novel core-shell structured ***β*-NaYF4:$Nd^{3+}$/$Yb^{3+}$/$Tm^{3+}$@NaYF4:$Nd^{3+}$@NaYF4@NaYF4:$Yb^{3+}$/$Er^{3+}$** UCNP (**Tm@Er**) possessing dual NIR excitations (808 and 980 nm) and the corresponding orthogonal emissions in the UV (347–475 nm)/visible (545 nm) range by using low power density excitation for minimal heating effects (Scheme 1). The unique photo-physical properties of these UCNPs represent a critical advance in many applications involving the construction of optical storage devices for information storage and transmission, developing advanced drug delivery systems which are capable of the sequential delivery of therapeutics, and multicolor bio-imaging and sensing. As a proof-concept experiment, we demonstrate the highly efficient two way photoswitching of spiropyran regulated by a single type of UCNP with dual NIR excitations.

The general structure of the UCNP contains a core and multiple shells, including a luminescent core (**LC**), an internal photon inert shell (**IS**) and an outer luminescent shell (**LS**) (Scheme 1a). In our developed UCNPs, the **LC** and **LS** contain different sensitizers and activators to generate orthogonal excitation and emission properties and the **IS** prevents energy migration between the two luminescent layers. Following this general design, $NaYF_4$ was chosen as the host matrix because of its low lattice phonon energies and high upconversion efficiency.[1d] We then doped the **LS** with $Yb^{3+}$ as a sensitizer, while co-doping the **LC** with both $Nd^{3+}$ and $Yb^{3+}$ (Scheme 1b). This specific arrangement of sensitizers affords an excitation of 980 nm to the UCNP **LS,** while the **LC** is responsive to both 980 nm and 808 nm excitations due to the separate main absorption peaks of $Yb^{3+}$ and $Nd^{3+}$ which locate at 980 and 808 nm, respectively.[8] It should be noted that $Nd^{3+}$ cannot transfer its excitation energy to activators directly. As such, it requires the use of $Yb^{3+}$ as a co-sensitizer, acting as an energy bridge.[8f–h] However, the presence of $Nd^{3+}$ in the **LC** not

only imbues the **LC** with 808 nm excitation, but also significantly decreases the upconversion luminescence (UCL) of the **LC** due to the enhanced cross-relaxation between $Nd^{3+}$ and locally positioned activators (quenching effect of $Nd^{3+}$,[8h] for more details see supporting information, Figure S1). As a result, the $Nd^{3+}$ doped **LC** becomes selectively excited underhigh power 808 nm excitation, with no emission observed from low power 980 nm excitation. Additionally, a layer of $NaYF_4$, without any dopant, was grown in between the **LC** and **LS,** as it can serve as a photon inert matrix which prevents energy migration between the **LC** and **LS**, which preserves their individual and spectrally pure excitation-emission properties.[9] As such, UCNPs with individual and orthogonal core-shell excitation-emission properties will be achieved, where the **LS** and **LC** will have individual emissions corresponding to individual excitations at 980 nm and 808 nm, respectively. Finally, $Tm^{3+}$ and $Er^{3+}$ were selected as activators of UCL due to their spectroscopic characteristics in the UV and visible region, respectively. In this work, two types of UCNPs were synthesized, henceforth abbreviated as **Tm@Er** UCNPs and **Er@Tm** UCNPs. **Tm@Er** UCNPs have $Tm^{3+}$ doped in the **LC** and $Er^{3+}$ doped in the **LS**, displaying UV-blue emission from the **LC** under 808 nm excitation and green emission from the **LS** under 980nm excitation. **Er@Tm** UCNPs have a reversed core-shell composition with regards to activator doping and therefore, reversed emissions. This difference in their emissive properties demonstrates the ability to orthogonally and selectively tune individual emissions based on the choice of activators of UCL (more details see main text discussion).

We first synthesized the **Tm@Er** core-shell UCNPs (Figure 1a). The UV-blue **LC** with 808 nm excitation was synthesized according to reported methods.[8g, h] It is comprised of a core (Figure 1b) doped with $Yb^{3+}$, $Nd^{3+}$, and $Tm^{3+}$, as well as a sensitized shell (Figure 1c) doped with $Nd^{3+}$ in high concentration. This core-shell structure minimizes the cross-relaxation between $Nd^{3+}$ and the local activators ($Tm^{3+}$) in the core due to the low $Nd^{3+}$ dopant concentration (1 mol%), but maximizes the absorption of 808 nm excitation in the shell due to the high $Nd^{3+}$ concentration (20%), endowing the nanoparticles with 808 nm excitation at low power density which minimizes local heating effects. As explained previously, to block the energy migration between the **LC** and **LS**, a layer of photon-inert $NaYF_4$ was further deposited *via* epitaxial growth (Figure 1d). Finally, a green colored **LS**, composed of $NaYF_4$:Yb/Er was deposited, led to a nanoparticle with a size of 41 nm × 52 nm (width × length, Figure. 1e). The shape evolution phenomena during the shell growth of the nanoparticles were ascribed to the kinetically favored anisotropic shell growth during the coating process, which was also observed by other groups.[8i, 10] The High-resolution TEM (HRTEM) image shown in Figure 1f reveals the (100) crystallographic planes of the **Tm@Er** UCNPs and demonstrates that the as-synthesized multishell UCNPs were single hexagonal phase crystals. Additionally, the energy-dispersive X-ray spectroscopy (EDX) spectrum indicates the presence of the elements Na, F, Y, Yb, Nd, Er, and Tm, which confirms the composition of the nanoparticles (see Supporting Information, Figure S2).

Next, we studied the upconversion profile of the as synthesized UCNPs under different wavelength laser excitations. As shown in Figure 2a, the **LC** of the **Tm@Er** UCNPs displays the characteristic emission peaks of $Tm^{3+}$ in the UV-blue region when excited using 808 and 980 nm lasers, due to the presence of $Nd^{3+}$ and $Yb^{3+}$ in the luminescent core.

Accordingly, a hexane solution of these core nanoparticles showed a deep blue colored band under 808 nm and 980 nm laser irradiation, which is easily seen by the naked eye (Figure 2a, right panel). For **Tm@Er**, only the characteristic emission peaks of $Tm^{3+}$ can be seen under 808 nm irradiation (Figure 2b, up curve), demonstrating the selective excitation of **LC** by 808 nm excitation. In contrast, the UCNPs display strong characteristic emissions from $Er^{3+}$ but relatively weak emissions from $Tm^{3+}$ under 980 nm excitation with a power density of 60 $W{\cdot}cm^{-2}$ (Figure 2b, bottom curve), indicating that both the **LC** and **LS** are excited as both of them use $Yb^{3+}$ as sensitizer. It should be noted that the relatively weaker emissions of $Tm^{3+}$ in **LC** than that of $Er^{3+}$ in **LS** may be due to i) the quenching effect of $Nd^{3+}$ in **LC**,[8h] and ii) the non-linear excitation nature of UCNPs whereby the UV emissions from $Tm^{3+}$ show a stronger dependence on excitation density than the visible emissions of $Er^{3+}$ (a 4 photon *vs* 3 photon process).[6b] Consequently, decreasing the excitation power density eliminated the $Tm^{3+}$ emissions more quickly than those of $Er^{3+}$, and excitations of 40 $W{\cdot}cm^{-2}$ or lower led to the selective emissions of $Er^{3+}$ in the **LS** only (Figure 2b, bottom curve). This result demonstrates that the emission of **Tm@Er** under 980 nm excitation can be easily modulated by regulating the excitation power/wavelength, and that the **LS** can be selectively excited by utilizing a low excitation power density due to the cooperative effect of the $Nd^{3+}$ doping, the photon inert shell and the nonlinear excitation properties of UCNPs,[6b, 6c, 11] as represented (Scheme 1b). Accordingly, a hexane solution of these nanoparticles displays two different colored bands, blue and green, under 808 nm and 980 nm excitation, respectively, with excitation power densities of 40 $W{\cdot}cm^{-2}$ or lower, revealing the orthogonal excitation-emission property of the **Tm@Er** UNCPs. Control experiments demonstrate that UCNPs with the same core-shell structure, but without the critical internal photon inert shell, display strong energy migration and do not possess separate core shell excitation-emission properties (Figure S3).

To further demonstrate the rationale behind the structure of the proposed UCNPs, another type of UCNP, **Er@Tm** was synthesized based on the inverse composition of the activators $Er^{3+}$ and $Tm^{3+}$ (Figure S4). In contrast to **Tm@Er** UNCPs, the **Er@Tm** UNCPs show incomplete separation of the core-shell excitations and emissions. Accordingly, 980 nm laser excitation stimulated not only UV-blue emissions from $Tm^{3+}$ in the **LS**, but also green emissions from $Er^{3+}$ in the **LC** (Figure S4f), indicating a simultaneous excitation of the luminescent core and shell by 980 nm irradiation at high power density. The relatively weaker emission from $Er^{3+}$ in the **LC** is mainly due to the quenching effect of $Nd^{3+}$ on locally placed activators. Decreasing the excitation power density can minimize the emission from $Er^{3+}$, but it will also result in decrease in UV emission from $Tm^{3+}$ (Figure S5). These results strongly suggest the rational design of the **Tm@Er** UCNPs, which have orthogonal core-shell excitation-emission properties at distinct wavelengths to yield spectrally pure UV-blue and green emissions. Furthermore, since 808 nm and low-power density 980 nm NIR light both minimize any local heating from the lasers (Figure S6), these UCNPs have unique advantages for applications in materials and biological studies, such as for driving important photoreactions with high spatiotemporal control and reversibly modulating the structure and properties of molecules such as photoswitches, especially for advancing multicolor UCNP based photoswitching systems which require distinct excitation-emission peaks, high photostability, and minimal photo-inducible damage.

UCNP based photoswitching systems, in which UCNPs serve as an antenna and deliver high energy UV-Vis light through the upconversion of low energy NIR light, are capable of the spatiotemporal and reversible modulation of the structure and properties of molecules.[6b, 6c, 6g, 11] Such systems can overcome the limitations of traditional UV-Vis light-based photoswitching, which include photobleaching, toxicity, and poor penetration through biological tissues. Spiropyran is one of the most well studied photoswitchable molecules known to date and is widely used in the development of photoswitches, molecular machines and sensors.[12] Biomolecules such as nucleic acids, enzymes, cellular receptors, and ion channels have been functionalized with **SP** to remotely and orthogonally regulate cellular behavior including gene transcription, enzyme activity, and flux through ion channels with light.[13] As illustrated in Scheme 1c, the photoisomerizations between spiropyran (**SP**) and merocyanine (**MC**) can be regulated by UV and visible light.[12a] Importantly, the maximum absorption peaks of **SP** and **MC** that locate at 342 nm and 560 nm, overlap well with the UV emission from the **Tm@Er** UCNPs under 808 nm excitation and the green emission of our **Tm@Er** UCNPs under 980 nm excitation, respectively (Figure 3b). As such, we sought to utilize this well-characterized photoswitch in our system to demonstrate the NIR light-based two-way photoswitching ability of the synthesized **Tm@Er** UCNPs (Figure 3a).

The photoswitching of **SP** by **Tm@Er** UCNPs was carried out using a simple mixture of **SP** and **Tm@Er** (more details see Figure S7). As shown in Figure 3b, irradiation of the colorless solution of **SP** and UCNPs with an 808 nm laser leads to the photo-isomerization of **SP** to **MC**, resulting in a bright pink solution which is characterized by a red shift in the UV peak as well as a dramatic enhancement in the absorption centered at 560 nm. These results indicate that the ring-opening reaction of the **SP** to **MC** was effectively driven by 808 nm excitation. Based on the kinetics monitoring of the photoswitching reaction using the characteristic absorption of **MC** at 560 nm (Figure 3c), 92 % of the photostationary state can be obtained within 120 seconds with 808 nm excitation with a power density of 40 $W \cdot cm^{-2}$. Thereafter, the NIR light driven photoisomerization of **MC** to **SP** was performed by irradiating the solution with a 980 nm laser. The solution quickly goes back to colorless and the absorption spectrum shows a blue shift in the UV absorption band and a decrease in intensity at 560 nm (Figure 3b). The kinetics of this photo reaction under 980 nm irradiation with **Tm@Er** UCNPs is much faster than those of the dark condition (Figure 3c). After 980 nm irradiation for 90 seconds with a power density of 15 $W \cdot cm^{-2}$ the absorption peak of **MC** no longer exists, indicating a complete photoisomerization reaction of **SP** to **MC**. These results demonstrate the successful two-way photoswitching of spiropyran, which is effectively driven using **Tm@Er** UNCPs with dual NIR excitations at low power density.

We further tested the integrity of SP photoswitching by using **Tm@Er** UCNPs with low power density 808 nm and 980 nm laser excitations, shown in Figure 3d. A schematic for the “remote control” two-way photoswitching of **SP** and the Tm@Er UNCPs by using two NIR lasers is shown in Figure 3a. It is worth noting that there is more than 90% retention of **SP** after 5 cycles of photoswitching, indicating the robustness and reversibility of our UNCP based photoswitching system which is mainly due to the attenuation of detrimental heating effects and photobleaching by using NIR light with low excitation power density. Finally,

we demonstrated the construction of mesoporous silica coated **Tm@Er** (UCNP@MSN), which allow the UCNPs to be easily dispersed in aqueous solutions and undergo facile surface chemistry for further functionalization and application (Figure S8).

In conclusion, we have successfully demonstrated the rational design and preparation of a new type of UCNP, which is capable of producing orthogonal and spectrally pure emissions from core-shell NIR excitations at low power density. In particular, the incorporation of two separate excitation triggers allows for a higher degree of control than achievable using previous systems. In contrast to previously reported photoswitch systems, our system excludes the necessity of high energy UV/Vis, as well as high power density NIR light, which attenuates any system damage from multi-photon absorption and local heating. Taken together, these results demonstrate that both our novel designed UCNP and UCNP-SP based NIR-driven two-way photoswitching platform has great implications for applications in materials science and biology studies.

## Supplementary Material

Refer to Web version on PubMed Central for supplementary material.

## Acknowledgments

We would like to acknowledge the kind support from Prof. Riman for fluorescent lifetime measurements. K.-B. Lee acknowledges financial support from the NIH Director's Innovator Award [1DP20D006462-01], National Institute of Biomedical Imaging and Bioengineering of the NIH [1R21NS085569-01], the N.J. Commission on Spinal Cord grant [09-3085-SCR-E-0], and the Rutgers Faculty Research Grant Program.

## References

1. a) Auzel F. Chem Rev. 2004; 104:139. [PubMed: 14719973] b) Wu SW, Han G, Milliron DJ, Aloni S, Altoe V, Talapin DV, Cohen BE, Schuck PJ. P Natl Acad Sci USA. 2009; 106:10917.c) Wang F, Han Y, Lim CS, Lu Y, Wang J, Xu J, Chen H, Zhang C, Hong M, Liu X. Nature. 2010; 463:1061. [PubMed: 20182508] d) Wang F, Deng R, Wang J, Wang QX, Han Y, Zhu H, Chen X, Liu X. Nat Mater. 2011; 10:968. [PubMed: 22019945] e) Wang F, Liu X. Chem Soc Rev. 2009; 38:976. [PubMed: 19421576] f) Wang J, Deng R, MacDonald MA, Chen B, Yuan J, Wang F, Chi D, Hor TSA, Zhang P, Liu G, Han Y, Liu X. Nat Mater. 2014; 13:157. [PubMed: 24270581] g) Haase M, Schafer H. Angew Chem Int Ed. 2011; 50:5808.
2. a) Li LL, Wu P, Hwang K, Lu Y. J Am Chem Soc. 2013; 135:2411. [PubMed: 23356394] b) Zhang Y, Zheng F, Yang T, Zhou W, Liu Y, Man N, Zhang L, Jin N, Dou Q, Zhang Y, Li Z, Wen LP. Nat Mater. 2012; 11:817. [PubMed: 22797828] c) Deng R, Xie X, Vendrell M, Chang Y, Liu X. J Am Chem Soc. 2011; 133:20168. [PubMed: 22107163] d) Gorris H, Ali R, Saleh SM, Wolfbeis OS. Adv Mater. 2011; 23:1652. [PubMed: 21472793] e) Nam SH, Bae YM, Park YI, Kim JH, Kim HM, Choi JS, Lee KT, Hyeon T, Suh YD. Angew Chem Int Ed. 2011; 50:6093.f) Huang X, Han S, Huang W, Liu X. Chem Soc Rev. 2013; 42:173. [PubMed: 23072924] g) Gorris HH, Wolfbeis OS. Angew Chem Int Ed. 2013; 52:3584.h) Sun L, Wang Y, Yan C. Acc Chem Res. 2014; 47:1001. [PubMed: 24422455] i) Yang Y, Shao Q, Deng R, Wang C, Teng X, Cheng K, Cheng Z, Huang L, Liu Z, Liu X, Xing B. Angew Chem Int Ed. 2012; 51:3125.j) Gu Z, Yan L, Tian G, Li S, Chai Z, Zhao Y. Adv Mater. 2013; 25:3758. [PubMed: 23813588] k) Liu Y, Zhou S, Tu D, Chen Z, Huang M, Zhu H, Ma E, Chen X. J Am Chem Soc. 2012; 134:15083. [PubMed: 22913455] l) Wang M, Mi CC, Wang WX, Liu CH, Wu YF, Xu ZR, Mao CB, Xu SK. ACS Nano. 2009; 3:1580. [PubMed: 19476317] m) Liu Q, Sun Y, Yang T, Feng W, Li C, Li F. J Am Chem Soc. 2011; 133:17122. [PubMed: 21957992] n) Yang J, Shen D, Li X, Li W, Fang Y, Wei Y, Yao C, Tu B, Zhang F, Zhao D. Chem –Eur J. 2012; 18:13642. [PubMed: 22996059]

3. a) Li W, Wang J, Ren J, Qu X. J Am Chem Soc. 2014; 136:2248. [PubMed: 24467474] b) Yan B, Boyer JC, Branda NR, Zhao Y. J Am Chem Soc. 2011; 133:19714. [PubMed: 22082025] c) Shen J, Chen G, Ohulchanskyy TY, Kesseli SJ, Buchholz S, Li Z, Prasad PN, Han G. Small. 2013; 9:3213. [PubMed: 23696330] d) Carling CJ, Nourmohammadian F, Boyer JC, Branda NR. Angew Chem Int Ed. 2010; 49:3782.
4. a) Idris NM, Gnanasammandhan MK, Zhang J, Ho PC, Mahendran R, Zhang Y. Nat Med. 2012; 18:1580. [PubMed: 22983397] b) Cui S, Yin D, Chen Y, Di Y, Chen H, Ma Y, Achilefu S, Gu Y. ACS Nano. 2013; 7:676. [PubMed: 23252747] c) Qiao XF, Zhou JC, Xiao JW, Wang YF, Sun LD, Yan CH. Nanoscale. 2012; 4:4611. [PubMed: 22706800] d) Wang C, Cheng L, Liu YM, Wang XJ, Ma XX, Deng ZY, Li YG, Liu Z. Adv Funct Mater. 2013; 23:3077.
5. a) Chen G, Ohulchanskyy TY, Kumar R, Agren H, Prasad PN. ACS Nano. 2010; 4:3163. [PubMed: 20509664] b) Dong NN, Pedroni M, Piccinelli F, Conti G, Sbarbati A, Ramirez-Hernandez JE, Maestro LM, Iglesias-de la Cruz MC, Sanz-Rodriguez F, Juarranz A, Chen F, Vetrone F, Capobianco JA, Sole JG, Bettinelli M, Jaque D, Speghini A. ACS Nano. 2011; 5:8665. [PubMed: 21957870]
6. a) Boyer JC, Carling CJ, Chua SY, Wilson D, Johnsen B, Baillie D, Branda NR. Chem –Eur J. 2012; 18:3122. [PubMed: 22344816] b) Boyer JC, Carling CJ, Gates BD, Branda NR. J Am Chem Soc. 2010; 132:15766. [PubMed: 20949969] c) Wang L, Dong H, Li Y, Xue C, Sun LD, Yan CH, Li Q. J Am Chem Soc. 2014; 136:4480. [PubMed: 24666208] d) Chen Z, Zhou L, Bing W, Zhang Z, Li Z, Ren J, Qu X. J Am Chem Soc. 2014; 136:7498. [PubMed: 24784766] e) Zhang F, Shi Q, Zhang Y, Shi Y, Ding K, Zhao D, Stucky GD. Adv Mater. 2011; 23:3775. [PubMed: 21766355] f) Zhang C, Xu CH, Sun LD, Yan CH. Chem -Asian J. 2012; 7:2225. [PubMed: 22987810] g) Zhang BF, Frigoli M, Angiuli F, Vetrone F, Capobianco JA. Chem Commun. 2012; 48:7244.
7. a) Zhan Q, Qian J, Liang H, Somesfalean G, Wang D, He S, Zhang Z, Andersson-Engels S. ACS Nano. 2011; 5:3744. [PubMed: 21513307] b) Jiang Z, Xu M, Li F, Yu Y. J Am Chem Soc. 2013; 135:16446. [PubMed: 24088066]
8. a) Qiu J, Kawamoto Y. J Appl Phys. 2002; 91:954.b) Courrol LC, Ranieri IM, Tarelho LVG, Baldochi SL, Gomes L, Vieira ND. J Appl Phys. 2005; 98:113504.c) Huang YL, Jang KH, Seo HJ, Jang KW. J Appl Phys. 2006; 100:83513.d) Koepke C, Wisniewski K, Sikorski L, Piatkowski D, Kowalska K, Naftaly M. Opt Mater. 2006; 28:129.e) Lupei A, Lupei V, Gheorghe C, Ikesue A, Osiac E. Opt Mater. 2009; 31:744.f) Wang YF, Liu GY, Sun LD, Xiao JW, Zhou JC, Yan CH. ACS Nano. 2013; 7:7200. [PubMed: 23869772] g) Xie X, Gao N, Deng R, Sun Q, Xu Q, Liu X. J Am Chem Soc. 2013; 135:12608. [PubMed: 23947580] h) Shen J, Chen GY, Vu AM, Fan W, Bilsel OS, Chang CC, Han G. Adv Opt Mater. 2013; 1:644.i) Wen H, Zhu H, Chen X, Hung TF, Wang B, Zhu G, Yu SF, Wang F. Angew Chem Int Ed. 2013; 52:13419.
9. Su Q, Han S, Xie X, Zhu H, Chen H, Chen C, Liu R, Chen X, Wang F, Liu X. J Am Chem Soc. 2012; 134:20849. [PubMed: 23210614]
10. Abel KA, Boyer JC, Andrei CM, van Veggel FCJM. J Phys Chem Lett. 2011; 2:185.b) Zhang C, Lee JY. ACS Nano. 2013; 7:4393. [PubMed: 23570424]
11. Liu J, Bu W, Pan L, Shi J. Angew Chem Int Ed. 2013; 52:4375.
12. a) Klajn R. Chem Soc Rev. 2014; 43:148. [PubMed: 23979515] b) Minkin VI. Chem Rev. 2004; 104:2751. [PubMed: 15137806]
13. a) Sakata T, Yan YL, Marriott G. P Natl Acad Sci USA. 2005; 102:4759.b) Ito Y, Sugimura N, Kwon OH, Imanishi Y. Nat Biotechnol. 1999; 17:73. [PubMed: 9920273] c) Beyer C, Wagenknecht HA. Synlett. 2010:1371.d) Kocer A, Walko M, Meijberg W, Feringa BL. Science. 2005; 309:755. [PubMed: 16051792]

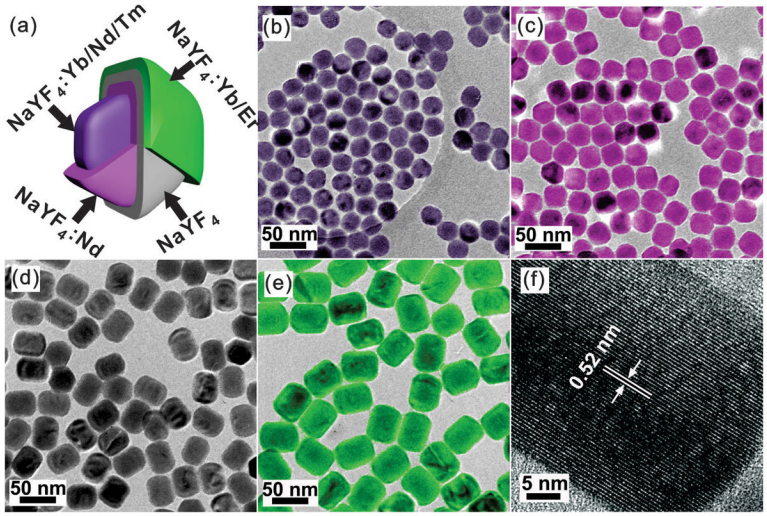


**FIGURE 1.**

(a) Composition of each layer of **Tm@Er** UCNPs. The false color of each layer represents the corresponding nanoparticles shown in b–e. (b–e) Low resolution TEM images of **Tm@Er** UCNPs constructed by epitaxial layer by layer growth. (f) High resolution TEM characterization of a single **Tm@Er** UCNP. The lattice extending, without interruption, across the particle is indicative of its single crystallinity.

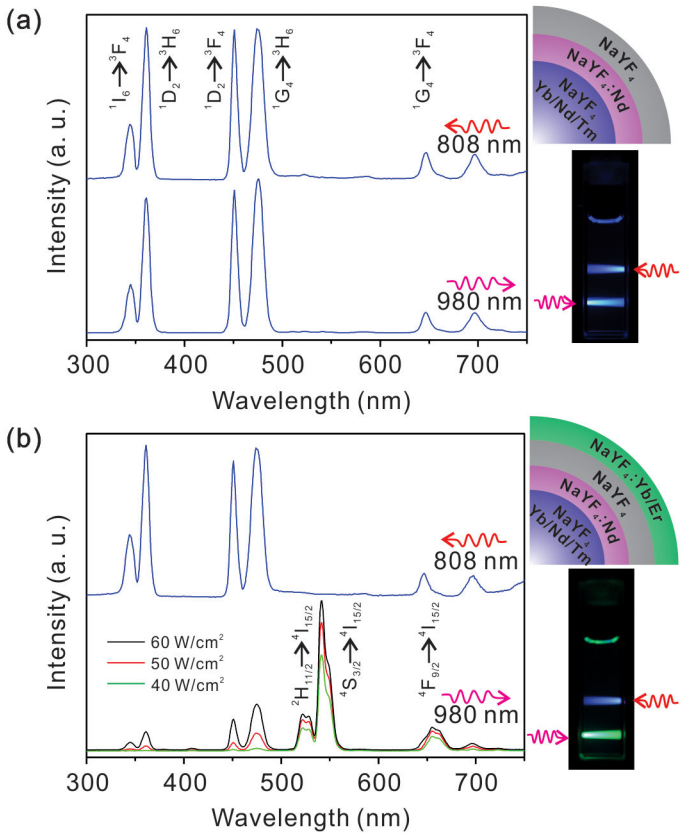


**FIGURE 2.**

Upconversion luminescence profiles of the luminescent core with photon inert shell (a) and the **Tm@Er** UCNPs (b) under different wavelength excitations and varying power densities. The structures of the corresponding nanoparticles are illustrated in the right panel. The photographs show the UCNPs in hexane solution (1 wt%) under irradiation from two laser beams with wavelengths of 808 nm and 980 nm. The power density for 808 nm and 980 nm lasers is 60 $W \cdot cm^{-2}$.

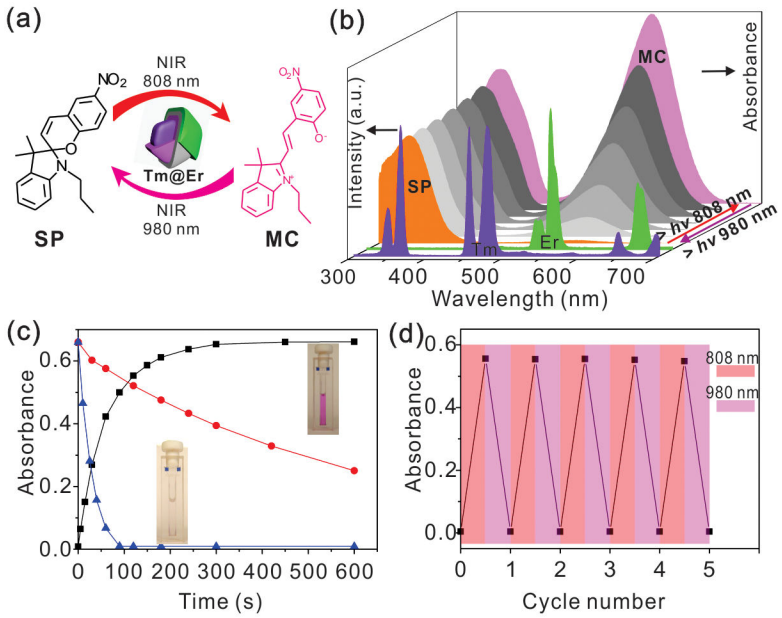


**FIGURE 3.**

(a) Schematic illustration of two-way photoswitching of **SP** by using **Tm@Er** UCNPs with dual NIR excitations. (b) $Tm^{3+}$ and $Er^{3+}$ emissions from **Tm@Er** nanoparticles under 808 nm and 980 nm excitations, respectively, which overlap well with the absorption peaks of **SP** and **MC**. The evolution of the UV/Vis absorption spectrum of the photoisomerization of **SP** and **MC** under 808 nm and 980 nm light irradiation in the presence of **Tm@Er** UCNPs. (c) Kinetic monitoring of the photoswitching reaction of **SP** and **MC** under 808 nm and 980 nm light irradiation with **Tm@Er** UCNPs by using the characteristic absorbance of **MC** at 560 nm. The red dotted line shows the kinetics of the reaction of **MC** to **SP** in dark conditions. (d) Dual NIR light-driven photoswitching of SP over many cycles in THF/methanol (9/1, v/v) solution with 5 wt% of **Tm@E**r UCNPs and 10 μM of **SP** by monitoring the absorbance of **MC** at 560 nm.

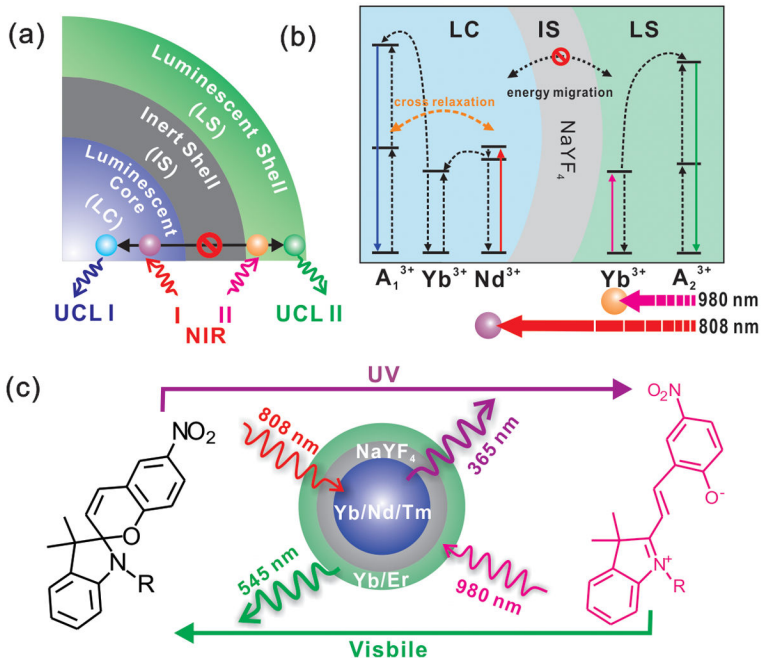


**SCHEME 1.**

(a) General structural design of the core-shell structured UCNPs. (b) Schematic illustration of the composition of the core-shell UCNPs and the simplified energy level diagram for the photon upconversion under NIR excitations. $Yb^{3+}$ was selectively co-doped with and without $Nd^{3+}$ into the **LC** and **LS** as a sensitizer, to endow the **LC** and **LS** with an excitation wavelength of 808 nm and 980 nm, respectively. Doping of $Nd^{3+}$ also leads to enhanced cross-relaxation between $Nd^{3+}$ and local activators, which quenches the UCL of the **LC** and thus endows the **LC** with a selective excitation of 808 nm with high power density. This structural design leads to orthogonal emissions in the luminescent core-shell under dual NIR excitations. (c) Direct and indirect two-way photoswitching of spiropyran by using UV/visible light and using **Tm@Er** UCNPs with dual NIR excitations.